



1

2 **The role of coccoliths in protecting *Emiliana huxleyi* against stressful light and**

3 **UV radiation**

4

5 **Running Title:** Photoprotective role of coccoliths in *Emiliana huxleyi*

6

7 Juntian Xu^{1,2}, Lennart T Bach³, Kai G Schulz³, Wenyan Zhao¹, Kunshan Gao^{1*}, Ulf

8 Riebesell³

9

10 ¹State Key Laboratory of Marine Environmental Science, Xiamen University, Xiamen,

11 Fujian, 361102 China;

12 ²Key Laboratory of Marine Biotechnology of Jiangsu Province, Huaihai Institute of

13 Technology, Lianyungang, Jiangsu, 222005 China;

14 ³GEOMAR Helmholtz Centre for Ocean Research Kiel, Düsternbrooker Weg 20, Kiel,

15 24105 Germany

16

17 *Author for Correspondence: ksgao@xmu.edu.cn (Kunshan Gao)

18

19

20

21

22



23 **Abstract**

24 Cocolithophores are a group of phytoplankton species which cover themselves
25 with small scales (coccoliths) made of calcium carbonate (CaCO_3). The reason why
26 coccolithophores form these calcite platelets has been a matter of debate since
27 decades but has remained elusive so far. One hypothesis is that they serve a role in
28 light/UV protection, especially in surface dwelling species like *Emiliana huxleyi*
29 which can tolerate exceptionally high levels of solar radiation. In this study, we tested
30 this hypothesis by culturing a calcifying and a non-calcifying strain under different
31 light conditions with and without UV radiation. The coccoliths of *E. huxleyi* reduced
32 the transmission of visible radiation (400-700 nm) by 7.5%, UV-A (315-400 nm) by
33 14.1% and UVB (280-315 nm) by 18.4%. Growth rates of the calcifying strain (PML
34 B92/11) were about 2 times higher than those of the non-calcifying strain (CCMP
35 2090) under indoor constant light levels in the absence of UV radiation. When
36 exposed to outdoor conditions (fluctuating sunlight with UV radiation), growth rates
37 of calcified cells were almost 3.5 times higher compared to naked cells. Furthermore,
38 relative electron transport rate was 114% higher and non-photochemical quenching
39 (NPQ) 281% higher in the calcifying compared to the non-calcifying strain, implying
40 higher energy transfer associated with higher NPQ in the presence of calcification.
41 When exposed to natural solar radiation including UV radiation, maximal quantum
42 yield of photosystem II was only slightly reduced in the calcifying but strongly
43 reduced in the non-calcifying strain. Our results reveal an important role of coccoliths
44 in mitigating light and UV stress in *E. huxleyi*.



45

46 **Key words:** coccoliths, *Emiliana huxleyi*, light protection, growth, photosynthetic

47 performance, UV radiation

48

49 **1 Introduction**

50 Coccolithophores are a group of marine phytoplankton species which are able to
51 precipitate CaCO₃ in the form of small calcitic scales (coccoliths) surrounding the
52 organic part of the cell. They contribute about by 1-10% to marine primary production
53 (Poulton et al., 2007) and approximately 50% to pelagic deep ocean CaCO₃ sediments
54 (Broecker and Clark, 2009). Blooms of coccolithophores can cover up to 8 million
55 km² of the Earth's surface (Moore et al., 2012), and are considered to be important
56 drivers of biogeochemical cycling (Rost and Riebesell, 2004).

57 Despite intense research on coccolithophore calcification and its biogeochemical
58 relevance during the last decade, it is still an unresolved question why
59 coccolithophores calcify (Young, 1994; Raven and Crawford, 2012). One hypothesis
60 is that the layer of coccoliths surrounding the cell (coccosphere) protects the organism
61 from excess light and UV radiation. This notion is supported by the exceptionally
62 high light tolerance of the surface layer dwelling species *Emiliana huxleyi* (Nanninga
63 and Tyrell, 1996; Gao et al., 2009).

64 Physiological studies investigating the light tolerance of *E. huxleyi* showed that the
65 radiation wavelength matters in this context. The coccosphere does not seem to
66 constitute a protection against very high intensities of photosynthetically active



67 radiation (PAR) since non-calcifying *E. huxleyi* cells are equally resistant to
68 photoinhibition as their calcifying counterparts (Nanninga and Tyrrell, 1996). This is
69 in clear contrast to the influence of stressful ultraviolet radiation (UVR) on the cells
70 where results from different physiological experiments support a protective role of the
71 coccoliths (Gao et al., 2009; Guan and Gao, 2010; Gao et al., 2012). Protection from
72 UVR or high light exposures by coccoliths may either work by physically shading
73 intracellular organelles or by facilitating thermal dissipation through increased
74 non-photochemical quenching (Xu and Gao, 2011). The underlying mechanisms,
75 however, are not well understood and warrant further investigations.

76 In this study we explore in more detail how different PAR and UV radiation
77 (280-400 nm) treatments affect calcifying and non-calcifying *E. huxleyi* cells.
78 Specifically we address the question whether the coccosphere of *E. huxleyi* helps the
79 cells to withstand stressful levels of PAR and/or UV radiation and whether
80 calcification influences photochemical performance.

81

82 **2. Materials and Methods**

83 **2.1 Materials and pre-culture conditions**

84 Calcifying *E. huxleyi* (PML B92/11 isolated in the Raunefjord area, Bergen,
85 Norway) and non-calcifying cells (CCMP 2090 isolated in the South Pacific) were
86 used in the experiments. Both strains were grown in triplicate cultures (300 ml square
87 glass bottles) at 15°C in 0.2 µm filtered natural seawater (gathered from the Gulf of
88 Biscay) at a photon flux density of 500 µmol photons m⁻² s⁻¹ on a 16/8 light/dark cycle.



89 The natural seawater medium was enriched with $64 \mu\text{mol L}^{-1}$ nitrate, $4 \mu\text{mol L}^{-1}$
90 phosphate, f/8 concentrations of a trace metal and vitamin mixture (Guillard & Ryther
91 1962), and 10 nmol kg^{-1} selenium. Pre-cultures and experimental incubations in
92 semi-continuously diluted batch cultures (>8 generations) ensured exponential growth
93 throughout the experiment.

94 2.2 Experimental setup

95 2.2.1 Indoor growth experiments

96 After pre-culture for at least 8 generations, the cells of calcifying and no-calcifying
97 strains were inoculated in the same glass bottles of 300 ml and cultured under the
98 same condition as pre-cultures, maintaining the cell concentrations at exponential
99 growth within a range of $3\text{-}10 \times 10^4$ cells/ml.

100 2.2.2 Outdoor growth experiments

101 Following the indoor growth experiment, the cells were transferred into quartz
102 tubes (100 ml) for the outdoor growth experiment and were exposed to natural solar
103 radiation at the institution's pier. The cultures were maintained outside in a
104 flow-through water tank, where the seawater temperature was maintained within a
105 range of $14\text{-}16^\circ\text{C}$. After the cells had acclimated for 7 days under the solar radiation,
106 aliquots of the cell cultures were transferred to new quartz tubes filled with fresh
107 medium before measurements were taken. For the outdoor cultures, the cells received
108 60% full spectrum solar radiation (the quartz tubes wrapped with neutral density
109 screens). The daytime average intensities (from 7:00 am to 5:00 pm) of PAR, UV-A



110 and UV-B which the cells received during the outdoor experiment were about 260
111 $\mu\text{mol photons m}^{-2} \text{ s}^{-1}$ (about 53 W m^{-2}), 12.4 and 0.34 W m^{-2} , respectively.

112 2.2.3 Short-term incubation experiments

113 Short-term incubation experiments were carried out to test UV effects around noon
114 time on a cloudy day and sunny day, respectively. Three different radiation treatments
115 were implemented as follows: 1) Cells in uncovered quartz tubes, receiving the full
116 spectrum of solar radiation (above 280 nm, PAB treatment); 2) cells in quartz tubes
117 covered with Folex 320 (Montagefolie, Nr. 10155099, Folex, Dreieich, Germany),
118 exposed to UV-A and PAR (above 320 nm, PA treatment); and 3) cells receiving only
119 PAR (P treatment) in quartz tubes covered with Ultraphan film 395 (UV Opak,
120 Digefra, Munich, Germany). The transmission spectra of the quartz tubes and the
121 cut-off foils are given by Zheng and Gao (2009). A time-course experiment was also
122 conducted around noon under full solar spectrum conditions.

123 2.3 Absorptivity of coccoliths

124 We examined absorption spectra of the cells with or without coccoliths to get an
125 indication on how much light and/or UV are blocked by the coccosphere. Therefore,
126 calcified cells (Cal-C), de-calcified cells (Cal-R, see above) and cells of the naked
127 strain (N-Cal) were filtered onto Whatman GF/F glass fiber filters (25 mm) which
128 were subsequently placed at the window near the detector of a double beam
129 UV-VIS-NIR spectrophotometer (PerkinElmer, Lambda950, USA). The absorption of
130 the GF/F filter was corrected with a control filter which was soaked with particle free
131 culture medium (Kishino et al., 1985).



132 2.4 Growth measurement

133 Cell densities were measured during a period of 7 days with a particle counter

134 (Coulter Z1, Beckman). The specific growth rate was calculated as: μ (d^{-1}) =

135 $(\ln N_t - \ln N_0)/t$, where N_0 and N_t represent the cell concentrations at the beginning and

136 the end of the incubations and t is the incubation time in days.

137 2.5 Chlorophyll fluorescence measurement

138 Parameters of *in vivo* induced chlorophyll a fluorescence of photosystem II were

139 estimated by a phyto-pulse amplitude modulated fluorometer (Phyto-PAM, Walz).

140 The maximum quantum yield of PSII (F_v/F_m) was calculated as: $F_v/F_m = (F_m -$

141 $F_o)/F_m$; where F_o is the basal fluorescence under measuring light of $0.2 \mu\text{mol}$

142 $\text{photons m}^{-2} \text{s}^{-1}$ and F_m the maximal fluorescence measured with a saturating light

143 pulse of $5000 \mu\text{mol photons m}^{-2} \text{s}^{-1}$ (0.8 s) in dark-adapted (15 min) cells.

144 In order to compare the transmission of the same strain with or without coccoliths

145 and to relate this to that of the non-calcifying strain, the calcified strain was

146 de-calcified with HCl (1 mol/L, the final concentration is 0.01 mol/L) for 10 s and

147 subsequent recovery of the pH with equimolar amounts of NaOH. Photochemical

148 performance was measured for dark-adapted (15 min) cells in calcified, de-calcified

149 or non-calcifying naked cells. De-calcified cells revealed F_v/F_m values similar to

150 those obtained prior to de-calcification. The actinic light levels were set at 533, 1077

151 and $2130 \mu\text{mol photons m}^{-2} \text{s}^{-1}$, respectively (growth light, saturated light and

152 over-saturated light). Non-photochemical quenching (NPQ) was calculated as: $\text{NPQ} =$

153 $(F_m - F_m')/F_m'$, where F_m was the maximum fluorescence yield after dark adaptation and



154 F_m' the maximum fluorescence yield under the actinic light levels.

155 To determine rapid light curves (RLCs, electron transport rate vs light), the cells
156 were exposed to 10 different PAR levels in sequence (87, 140, 263, 382, 449, 611, 778,
157 993, 1195 and 1391 $\mu\text{mol photons m}^{-2} \text{s}^{-1}$), each of which lasted for 20 s. The relative
158 electron transport rate (rETR) was assessed as: $\text{rETR} = \text{Yield} \times 0.5 \times \text{PFD}$, where the
159 yield represents the effective quantum yield of PSII (F_v'/F_m'); the coefficient 0.5 takes
160 into account that roughly 50% of all absorbed quanta reach PSII; and PFD is the
161 photon flux density of the actinic light ($\mu\text{mol m}^{-2} \text{s}^{-1}$) (Genty et al., 1989).

162 To examine immediate photochemical responses of the cells to UV radiation, the
163 cells were exposed to the three different solar radiations (see above) for 60 min during
164 noontime under natural solar radiation. The effective quantum yield was calculated as:
165 $F_v'/F_m' = (F_m' - F_t) / F_m'$, where F_m' and F_t are the maximal fluorescence and steady
166 state fluorescence in the light adapted cells, respectively.

167 2.6 Measurement of solar irradiances

168 Solar PAR was measured using a Quantum Scalar Laboratory Irradiance Sensor
169 (QSL-2100/ 2101, Biospherical Instruments, San Diego, USA). The measured values
170 were recorded every 10 s and saved on a computer. Solar UV-A and UV-B radiation
171 were measured with a radiometer (PMA 2100 Solar Light Co., Glenside, USA), the
172 mean irradiances of solar UV-A and UV-B during the experimental periods were
173 confirmed according to the ratios of UV-A/UV-B to PAR at the experimental location.

174 2.7 Statistics

175 The data were expressed as the means \pm standard deviation (SD). Statistical



176 significance of the data was tested with software of Origin 9.0 (one way ANOVA,
177 Tukey's post-hoc test). A confidence level of 95% was used in all analyses.

178

179 **3 Results**

180 The coccolith layer of *E. huxleyi* absorbed both visible and UV radiation. It reduced
181 the transmission of visible radiation (400-700 nm) by 7.5%, UV-A (315-400 nm) by
182 14.1% and UVB by 18.4% (280-315 nm) relative to decalcified cells and 6.5% for
183 PAR, 6.6% for UV-A and 5.1% for UV-B, relative to non-calcifying cells (Fig. 1). The
184 specific growth rate of calcifying *E. huxleyi* strain (PML B92/11) was about 2 times
185 higher than that of the non-calcifying strain (CCMP 2090) ($P < 0.05$) when grown at
186 $500 \mu\text{mol photons m}^{-2} \text{ s}^{-1}$ of PAR under indoor conditions (Fig. 2A). Growth rates of
187 both strains were significantly ($P < 0.05$) reduced when the cells were transferred
188 outdoor and exposed to natural solar radiation. However, under outdoor conditions,
189 growth rates of calcified cells were 3.5 times higher than those of the non-calcifying
190 cells, indicating that the latter was more harmed by the solar exposure than the former
191 (Fig. 2A). The cell diameter was not significantly different in the calcified cells
192 between the indoor and outdoor conditions ($P > 0.05$), but an 18% increase was found
193 in the non-calcifying cells after they had grown under the outdoor conditions for 7
194 days ($P < 0.05$) (Fig. 2B). The maximal quantum yield (Fv/Fm) decreased when the
195 cells were transferred from indoor to the outdoor conditions, reflecting a harmful
196 effect of solar radiation. The decrease of Fv/Fm, however, was much more
197 pronounced in the non-calcifying cells (27%) compared to calcifying cells (11%) (Fig.



198 2C).

199 Calcified cells had significantly higher rETR, higher apparent light use efficiency
200 (α), and higher maximal electron transport rate (rETR_{max}), but significantly lower
201 light saturation parameters (I_k). The de-calcified cells of the calcifying strain showed
202 a remarkable decrease of rETR_{max} ($P < 0.05$), but did not show obvious changes in α
203 and I_k (Fig. 3, Table 1). Increased actinic light levels (acclimating light during the
204 fluorescence measurement) led to higher NPQ in both the calcifying and
205 non-calcifying strain (Fig. 4). Furthermore, calcified cells showed higher NPQ values
206 compared to non-calcifying cells ($p < 0.05$).

207 When exposed to full spectrum solar radiation, the quantum yield of calcified cells
208 showed no significant change during the first 30 min ($P > 0.05$). After 30 minutes,
209 quantum yield quickly dropped from about 0.35 to 0.22 for ~20 min ($P < 0.05$)
210 followed by a slight recovery in the last 25 minutes. A similar trend was observed in
211 the de-calcified cells with the key difference that the sharp decrease already happened
212 during the first 10 min. Quantum yield of the non-calcifying cells decreased
213 constantly for the first 50 minutes and remained at the low level thereafter (Fig. 5).

214 No effect of the radiation treatment (P, PA and PAB radiation) on the quantum yield
215 of calcified cells was observed after the cells grown under indoor condition were
216 transferred to outdoor solar radiation for 1h exposure (very cloudy day, average PAR,
217 UV-A and UV-B were 481 $\mu\text{mol photons m}^{-2} \text{s}^{-1}$, 22.1 and 0.7 W m^{-2} , respectively) ($P >$
218 0.05). Quantum yield was significantly higher in the non-calcifying cells, however,
219 when they were exposed to UVA radiation (PA vs. P treatment, $P < 0.05$ Fig. 6A).



220 Similar responses were observed when the same test was done on a sunny day with
221 average PAR, UV-A and UV-B of 1605 $\mu\text{mol photons m}^{-2} \text{ s}^{-1}$, 69 and 2.4 W m^{-2} ,
222 respectively. Here, the quantum yield of the calcified cells showed no significant
223 difference between the different light treatments but it decreased significantly under
224 PAB treatment compared to P treatments in the non-calcifying cells ($P < 0.05$) (Fig.
225 6B).

226

227 4 Discussion

228 Various hypotheses were proposed for the possible functions of coccoliths, but none
229 of them is supported by sufficient evidence (Young, 1994; Raven and Crawford,
230 2012). One important function of coccoliths for surface-dwelling species such as *E.*
231 *huxleyi* could be the protection against high photon flux densities, especially UV
232 radiation (Berge, 1962; Young, 1994; Gao et al., 2009).

233 Some of our results support this hypothesis. The growth rate of the calcified cells of
234 *E. huxleyi* grown under indoor conditions was about 2 times higher than that of naked
235 cells. This difference came out even stronger, with growth rates 3.5 times higher in
236 calcified versus naked cells, when the cells were exposed to full spectrum solar
237 radiation (Fig. 2A). This could potentially be attributed to the screening of PAR,
238 UV-A, and UV-B by coccoliths. Although the daytime PAR of solar radiation was
239 reduced to about half of the light level of the indoor test, noon time PAR levels were
240 higher than 500 $\mu\text{mol photons m}^{-2} \text{ s}^{-1}$, and the presence of UV could lead to more
241 harms to the naked cells. Light protection by coccoliths is further supported by the



242 Fv/Fm measurements. The maximum photochemical efficiency of PSII was only
243 slightly reduced in calcified cells but significantly decreased in non-calcifying cells
244 when they were exposed to natural solar PAR and UV radiation (Fig. 2C).
245 Furthermore, photochemical performance of de-calcified cells decreased significantly
246 faster and stronger with time compared calcified cells (Fig. 5).

247 The diameter of calcified cells did not significantly change when they were
248 exposed to the full spectrum of solar radiation. The diameter of the non-calcifying
249 cells, however, increased significantly (Fig. 2B). Perhaps, the non-calcifying cells
250 experienced more DNA damage and so did not enter the S phase regularly (Buma et
251 al., 2000). Alternatively, it may reflect a strategy to acclimatize to stressful solar UV
252 radiation since it is well known that smaller cells are usually more sensitive to UV
253 than their larger counterparts (Garcia-Pichel, 1994; Laurion and Vincent, 1998). Some
254 field and laboratory studies showed increased cell size with increased UV exposures
255 (Buma et al., 2000), which can be interpreted as adaptive or acclimation mechanism
256 for protecting the cells against UV radiation.

257 Several studies found that coccoliths do not protect *E. huxleyi* from excess PAR
258 (Nanninga and Tyrrell, 1996; Houdan et al., 2005; Trimborn et al., 2007). However,
259 UV radiation was not considered in these experiments. Our results showed that the
260 non-calcifying cells were more sensitive to full spectrum solar radiation than calcified
261 cells and even in the same strain, the photochemical performance of de-calcified cells
262 decreased significantly when comparing the calcified cells. This suggests that
263 coccoliths efficiently protect the cells from solar UV radiation.



264 On the other hand, *E. huxleyi* appears to be more sensitive to UV-B irradiances than
265 other phytoplankton species, and its growth rate and physiological performances were
266 highly inhibited by UV radiation (Peletier et al., 1996; Buma et al., 2000; Xu et al.,
267 2011). However, competition tests for community changes are rare, and longer-term
268 experiments with less extreme UVR would be more ecologically and evolutionarily
269 relevant (Raven and Crawford, 2012). In our work, UVR had no significant effect on
270 the quantum yield of calcified cells regardless of high or low light condition but it
271 showed inhibition in non-calcifying cells when they were exposed to high solar light
272 (Fig. 6A, B). This provides further evidence for protection by coccoliths against UV
273 radiation.

274 On the cloudy day, no significant difference was observed among the treatments for
275 the calcifying cells; on the sunny day, under the fluctuating light (data not shown)
276 calcifying cells manage to refurbish damage to their photosynthetic apparatus by
277 balancing damage and repair (Gao et al., 2007). For the non-calcifying cells, on the
278 other hand, UV damage was not effectively repaired, leading to the observed negative
279 effect on photosynthetic performance.

280 In conclusion, the coccoliths of calcifying *E. huxleyi* play an important role in
281 protecting this species against harmful solar radiation especially UV-A and UV-B .
282 The reported absence of photoinhibition in this alga at high light levels is most likely
283 connected to the photoprotective role played by the coccosphere of *E. huxleyi*. With
284 shoaling of the upper mixed layer (UML) caused by global warming and progressive
285 ocean acidification, reduced thickness or the number of coccoliths (Gao et al., 2009;



286 De Bodt et al., 2010), cells of *E. huxleyi* living within the UML would be impacted
287 due to increased daily exposures to solar radiation.

288

289 **Acknowledgements**

290 This study was supported by National Natural Science Foundation (41430967;
291 41476097; 41120164007), State Oceanic Administration (National Programme on
292 Global Change and Air-Sea Interaction, GASI-03-01-02-04), Joint project of National
293 Natural Science Foundation of China and Shandong province (No. U1406403),
294 Strategic Priority Research Program of Chinese Academy of Sciences (No.
295 XDA1102030204). Visit of KG to Kiel was supported by DAAD.

296

297 **References**

- 298 Berge, G.: Discoloration of the sea due to *Coccolithus huxleyi* “bloom”, *Sarsia*, 6,
299 27-40, 1962.
- 300 Broecker, W., and Clark, E.: Ratio of coccolith CaCO_3 to foraminifera CaCO_3 in late
301 Holocene deeper-sea sediments, *Paleoceanography*, 24, PA3205, 2009
- 302 Buma, A. G. J., van Oijen, T., van de Poll, W., Veldhuis, M. J. W., and Gieskes, W.
303 W. C.: The sensitivity of *Emiliana huxleyi* (Prymnesiophyceae) to ultraviolet-B
304 radiation, *J. Phycol.*, 36, 296-303, 2000.
- 305 De Bodt, C., Van Oostende, N., Harlay, J., Sabbe, K., and Chou, L.: Individual and
306 interacting effects of pCO_2 and temperature on *Emiliana huxleyi* calcification:
307 study of the calcite production, the coccolith morphology and the coccosphere



- 308 size, *Biogeosciences*, 7, 1401-1412, 2010.
- 309 Gao, K., Ruan, Z., Villafane, V. E., Gattuiso, J. P., and Helbling, E. W.: Ocean
310 acidification exacerbates the effect of UV radiation on the calcifying
311 phytoplankter *Emiliana huxleyi*, *Limnol. Oceanogr.*, 54, 1855-1862, 2009.
- 312 Gao, K., Helbling, E. W., Häder, D. P., and Hutchins, D. A.: Responses of marine
313 primary producers to interactions between ocean acidification, solar radiation,
314 and warming, *Mar. Ecol. Prog. Ser.*, 470, 167-189, 2012.
- 315 Gao, K., Wu, Y., Li, G., Wu, H, Villafañe, V. E., and Helbling, E. W.: Solar UV
316 radiation drives CO₂ fixation in marine phytoplankton: A double-edged sword.
317 *Plant Physiol.*, 144, 54-59, 2007.
- 318 Garcia-Pichel, F.: A model for internal self-shading in planktonic organisms and its
319 implications for the usefulness of ultraviolet sunscreens, *Limnol. Oceanogr.*, 39,
320 1704-1717, 1994.
- 321 Genty, B., Briantais, J. M., and Baker, N. R.: The relationship between the quantum
322 yield of photosynthetic electron-transport and quenching of chlorophyll
323 fluorescence, *Biochim. Biophys. Acta*, 990, 87-92, 1989.
- 324 Guan, W., and Gao, K.: Enhanced calcification ameliorates the negative effects of UV
325 radiation on photosynthesis in the calcifying phytoplankter *Emiliana*
326 *huxleyi*, *Chin. Sci. Bull.* 55, 588-593, 2010.
- 327 Guillard, R. R., and Ryther, J. H.: Studies of marine planktonic diatoms: I. *Cyclotella*
328 *nana* hustedt, and *Detonula confervacea* (cleve) gran, *Can. J. microbial.*, 8,
329 229-239, 1962.



- 330 Houdan, A., Probert, I., Van Lenning, K., and Lefebvre, S.: Comparison of
331 photosynthetic responses in diploid and haploid life-cycle phases of *Emiliana*
332 *huxleyi* (Prymnesiophyceae), Mar. Ecol. Prog. Ser., 292:139-146, 2005.
- 333 Kishino, M., Takahashi, M., Okami, N., and Ichimur S.: Estimation of the spectral
334 absorption coefficients of phytoplankton in the sea, Bull. Mar. Biol., 37: 634-642,
335 1985.
- 336 Laurion, I., and Vincent, W. F.: Cell size versus taxonomic composition as
337 determinants of UV-sensitivity in natural phytoplankton communities, Limnol.
338 Oceanogr., 43, 1774-1779, 1998.
- 339 Moore, T. S., Dowell, M. D., and Franz, B. A.: Detection of coccolithophore blooms
340 in ocean color satellite imagery: a generalized approach for use with multiple
341 sensors, Remote Sens. Environ., 117, 249-263, 2012.
- 342 Nanninga, H. J., and Tyrrell, T.: Importance of light for the formation of algal blooms
343 by *Emiliana huxleyi*, Mar. Ecol. Progr. Ser., 136, 195-203, 1996.
- 344 Peletier, H., Gieskes, W. W. C., and Buma, A. G. J.: Ultraviolet-B radiation resistance
345 of benthic diatoms isolated from tidal flats in the Dutch Wadden Sea, Mar. Ecol.
346 Prog. Ser., 135, 163-168, 1996.
- 347 Poulton, A. J., Adey, T. R., Balch, W. M., and Holligan, P. M.: Relating
348 coccolithophore calcification rates to phytoplankton community dynamics:
349 regional differences and implications for carbon export, Deep-Sea Res. Part II,
350 54, 538-557, 2007.
- 351 Raven, J. A., and Crawford, K.: Environmental controls on coccolithophore



352 calcification, Mar. Ecol. Progr. Ser., 470, 137-166, 2012.

353 Rost, B., and Riebesell, U.: Coccolithophores and the biological pump: responses to
354 environmental changes, In: Coccolithophores- from molecular processes to
355 global impact, Thierstein, H. R., and Young, J. R. (eds), Springer, Berlin,
356 99-125, 2004.

357 Trimborn, S., Langer, G., and Rost, B.: Effect of varying calcium concentrations and
358 light intensities on calcification and photosynthesis in *Emiliana huxleyi*, Limnol.
359 Oceanogr., 52, 2285-2293, 2007.

360 Xu, K., Gao, K., Villafane, V. E., Helbling, E. W.: Photosynthetic responses of
361 *Emiliana huxleyi* to UV radiation and elevated temperature: roles of calcified
362 coccoliths, Biogeosciences, 8, 1441-1452, 2011.

363 Young, J. R.: Functions of coccoliths, In: Coccolithophores, Winter, A., and Siesser,
364 W. G. (eds), Cambridge University Press, Cambridge, 63-82,1994.

365 Zheng, Y., and Gao, K.: Impacts of solar UV radiation on the photosynthesis, growth,
366 and UV-absorbing compounds in *Gracilaria lemaneiformis* (Rhodophyta) grown
367 at different nitrate concentrations, J. Phycol., 45, 314-323, 2009.

368

369 **Figure captions**

370 **Figure 1.** Transmission spectra of cells with (Cal-C, calcifying strain) and without
371 (Cal-R, calcifying strain with coccoliths removed artificially) coccolith cover and
372 non-calcifying (N-Cal) cells of *Emiliana huxleyi*.

373

374 **Figure 2.** The specific growth rate (μ) (A), diameter (B) and maximum quantum yield



375 (C) of PSII (Fv/Fm) of the calcified (Cal-C) and non-calcifying (N-Cal) cells of *E.*
376 *huxleyi* grown in indoor and outdoor conditions. Different letters represent significant
377 difference between the indoor and outdoor experiments. Different horizontal lines
378 represent significant difference between the different strains.

379

380 **Figure 3.** The relative electron rate (rETR) of coccolith-covered (Cal-C),
381 coccolith-removed (Cal-R) and non-calcifying (N-Cal) cells of *E. huxleyi* grown
382 under indoor conditions as function of PAR. The cells had been grown for 12-22
383 generations under $500 \mu\text{mol photons m}^{-2} \text{ s}^{-1}$ of PAR.

384

385 **Figure 4.** The non-photochemical quenching (NPQ) of coccolith-covered (Cal-C) and
386 non-calcifying (N-Cal) cells of *E. huxleyi* grown under indoor conditions. Different
387 letters represent significant difference among the light levels. Different horizontal
388 lines represent significant difference among the different type cells.

389

390 **Figure 5.** The time course of quantum yield of coccolith-covered (Cal-C),
391 coccolith-removed (Cal-R) and non-calcifying (N-Cal) cells of *E. huxleyi* under full
392 spectrum solar radiation (noontime, average PAR, UV-A and UV-B were $1082 \mu\text{mol}$
393 $\text{photons m}^{-2} \text{ s}^{-1}$, 48.1 and 1.6 W m^{-2} , respectively).

394

395 **Figure 6.** The change of quantum yield of the calcified (Cal-C) and non-calcifying
396 (N-Cal) cells of *E. huxleyi* when transferred from indoor to outdoor conditions, being
397 exposed to PAR alone (P), PAR+UVA(PA) and PAR+UVA+B(PAB) for 60 min at
398 around noon time. A, measured under a cloudy day (average PAR, UV-A and UV-B
399 were $481 \mu\text{mol photons m}^{-2} \text{ s}^{-1}$, 22.1 and 0.7 W m^{-2} , respectively); B, measured under



400 a sunny day (average PAR, UV-A and UV-B were $1605 \mu\text{mol photons m}^{-2} \text{s}^{-1}$, 69 and
401 2.4 W m^{-2}). Different letters represent significant difference among the light
402 treatments. Different horizontal lines represent significant difference between the
403 different strains.

404

405

406

407

408

409

410

411

412

413

414

415

416

417

418

419

420

421

422

423

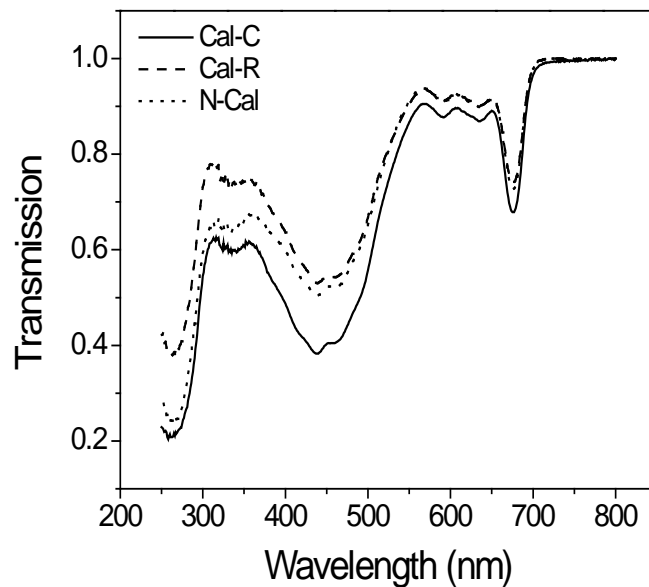


424 Table 1. Photosynthetic parameters of relative electron transport rate (Figure 3) as a
425 function of PAR, different letters represent significant difference ($P < 0.05$) among the
426 treatments.

	α	$rETR_{\max}$	I_k
Cal-C	0.23 ± 0.02^a	90.6 ± 9.0^a	1010.8 ± 95.0^a
Cal-R	0.20 ± 0.01^a	73.5 ± 3.5^b	986.3 ± 27.4^a
N-Cal	0.17 ± 0.02^b	42.3 ± 8.5^c	621.8 ± 111.1^b



427



428

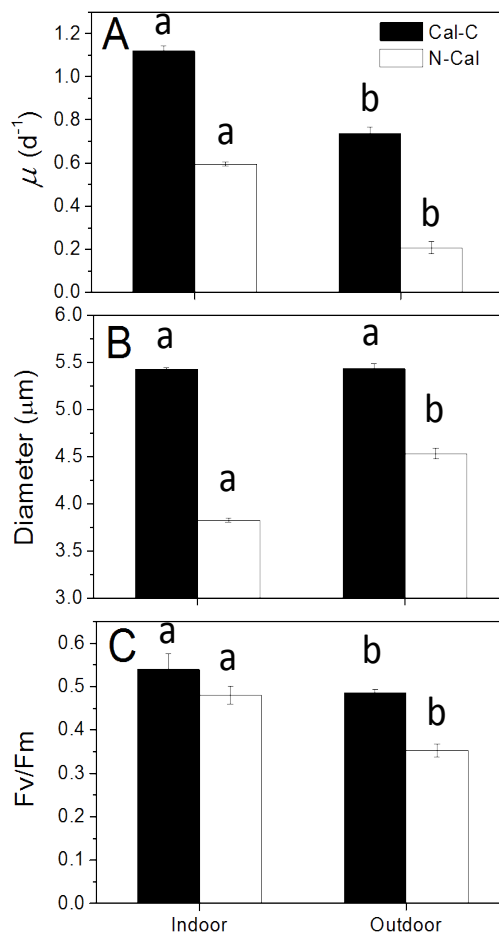
429

430

431

Fig. 1

432



433

434

435

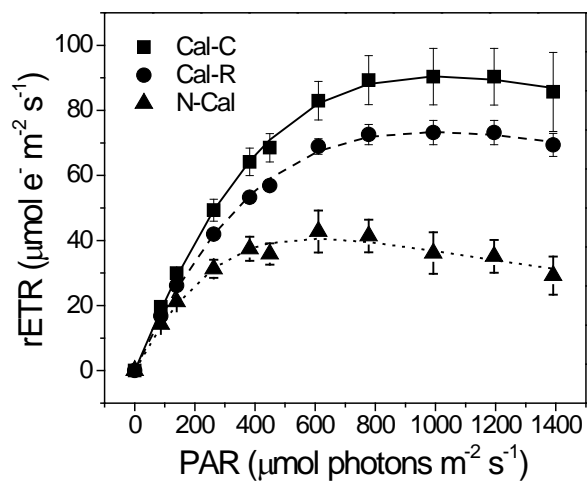
436

437

438

439

Fig. 2



440

441

442

443

Fig. 3

444

445

446

447

448

449

450

451

452

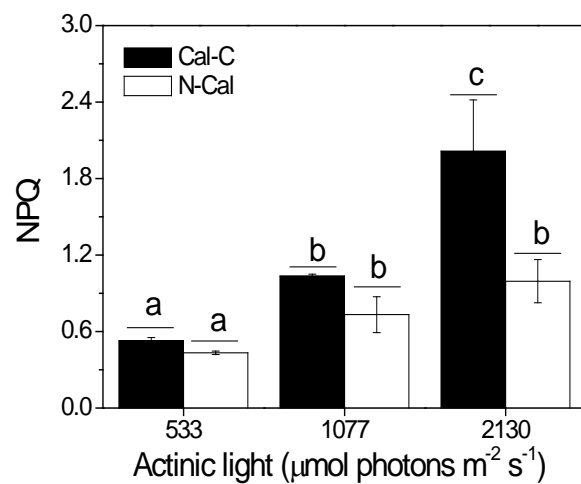
453

454



455

456



457

458

459

460

461

Fig. 4

462

463

464

465

466

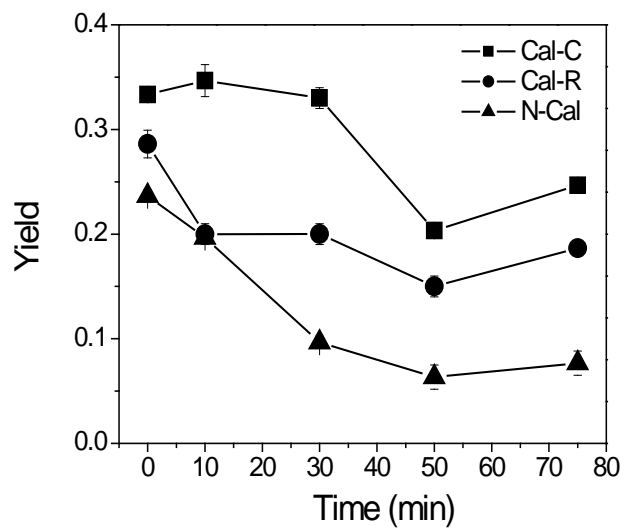
467

468

469



470



471

472

473

474

Fig. 5

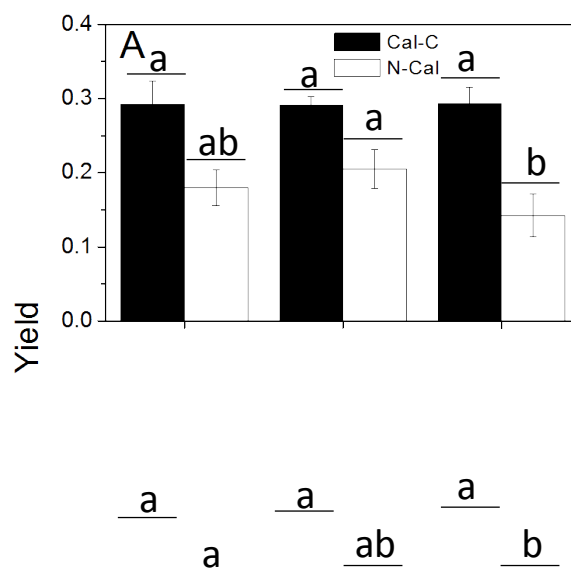
475

476

477

478

479



480

481

482

Fig. 6

483

484

485

486

487

488

489